International Journal of Nanomedicine

Dovepress
open access to scientific and medical research

Open Access Full Text Article

ORIGINAL RESEARCH

Dually Active Apigenin-Loaded Nanostructured Lipid Carriers for Cancer Treatment

Lorena Bonilla-Vidal[1,2], Marta Świtalska[3], Marta Espina[1,2], Joanna Wietrzyk[3], Maria Luisa García[1,2], Eliana B Souto[4,5], Anna Gliszczyńska[6,*], Elena Sánchez López[1,2,7,*]

[1]Department of Pharmacy, Pharmaceutical Technology and Physical Chemistry, University of Barcelona, Barcelona, Spain; [2]Institute of Nanoscience and Nanotechnology (IN^{2}UB), University of Barcelona, Barcelona, Spain; [3]Department of Experimental Oncology, Ludwik Hirszfeld Institute of Immunology and Experimental Therapy, Polish Academy of Sciences, Wrocław, Poland; [4]Laboratory of Pharmaceutical Technology, Department of Drug Sciences, Faculty of Pharmacy, University of Porto, Porto, Portugal; [5]Associate Laboratory i4HB—Institute for Health and Bioeconomy, Faculty of Pharmacy, University of Porto, Porto, Portugal; [6]Department of Food Chemistry and Biocatalysis, Wrocław University of Environmental and Life Sciences, Wrocław, Poland; [7]Unit of Synthesis and Biomedical Applications of Peptides, IQAC-CSIC, Barcelona, Spain

*These authors contributed equally to this work

Correspondence: Elena Sánchez López; Anna Gliszczyńska, Email esanchezlopez@ub.edu; anna.gliszczynska@upwr.edu.pl

Purpose: Cancer is one of the major causes of death worldwide affecting more than 19 million people. Traditional cancer therapies have many adverse effects and often result in unsatisfactory outcomes. Natural flavones, such as apigenin (APG), have demonstrated excellent antitumoral properties. However, they have a low aqueous solubility. To overcome this drawback, APG can be encapsulated in nanostructured lipid carriers (NLC). Therefore, we developed dual NLC encapsulating APG (APG-NLC) with a lipid matrix containing rosehip oil, which is known for its anti-inflammatory and antioxidant properties.

Methods: Optimisation, physicochemical characterisation, biopharmaceutical behaviour, and therapeutic efficacy of this novel nanostructured system were assessed.

Results: APG-NLC were optimized obtaining an average particle size below 200 nm, a surface charge of −20 mV, and an encapsulation efficiency over 99%. The APG-NLC released APG in a sustained manner, and the results showed that the formulation was stable for more than 10 months. In vitro studies showed that APG-NLC possess significant antiangiogenic activity in ovo and selective antiproliferative activity in several cancer cell lines without exhibiting toxicity in healthy cells.

Conclusion: APG-NLC containing rosehip oil were optimised. They exhibit suitable physicochemical parameters, storage stability for more than 10 months, and prolonged APG release. Moreover, APG-NLC were internalised inside tumour cells, showing the capacity to cause cytotoxicity in cancer cells without damaging healthy cells.

Keywords: antitumoral, lipid nanoparticles, apigenin, rosehip oil

Introduction

Cancer is one of the leading causes of death worldwide. In 2020, there were almost 19 million patients, and almost 10 million deaths were attributed to cancer.[1,2] Traditional therapies such as chemotherapy and radiotherapy have many adverse effects and unsatisfactory treatment outcomes.[3,4] Particularly, it has been estimated that over 50% of cancer patients usually receive chemotherapy at some stage of their disease.[5] However, most existing cancer therapies simultaneously affect healthy and tumour cells, resulting in significant adverse effects.[6–8] In addition, these therapies can lead to chemoresistance. Therefore, the development of novel therapeutic strategies is an unmet medical need.[9–11]

In recent years, herbal medicines have gained wide attention owing to their beneficial effects against various diseases such as cancer.[12,13] Apigenin (APG) is a plant-derived flavone that possesses interesting properties, particularly potent antitumour activity. It has been reported that APG possesses antitumour activity against different types of cancer by triggering apoptosis, inducing autophagy, modulating the cell cycle, decreasing cell motility, inhibiting cancer cell migration and evasion, and stimulating the immune response.[14–16] Despite being a highly effective molecule that acts

Received: 5 August 2023
Accepted: 24 October 2023
Published: 23 November 2023

on many mechanisms inside the cell, its main problem is low bioavailability because of its poor water solubility and metabolization in the intestine and liver.[5,17]

In recent years, pharmaceutical research has focused on the development of nanotechnological systems applied in different fields, with special relevance to drug delivery.[18] Nanocarriers can be designed to deliver drugs into specific tissues. These nanocarriers can overcome the limitations of conventional treatments by enhancing drug solubility, improving pharmacokinetics, increasing efficacy, and reducing adverse effects. In particular, nanoparticles for cancer therapy constitute a highly interesting alternative because of the possibility of establishing passive targeting, since tumoural cell properties allow them to selectively accumulate in these cells due to their enhanced permeability and retention.[19,20] Among several nanocarriers, lipid nanoparticles and nanostructured lipid carriers (NLC) have gained attention because of their ability to encapsulate both lipophilic and hydrophilic drugs, employment of biocompatible lipids, prolonged drug release, and easy scale-up.[21–23]

To increase the solubility of APG promoting an improvement of its bioavailability, in the present work we developed APG-loaded NLC for the treatment of different types of tumors. Moreover, rosehip oil, a natural compound extracted from the seeds of wild roses, was chosen as the liquid lipid owing to its pharmaceutical properties. Rosehip oil has traditionally been used for dermal applications as a skin regenerator and possesses anti-inflammatory and antioxidant effects. Furthermore, recent studies indicate that rosehips contain active compounds with antitumoral activity.[24,25] These properties might result in a synergic way between the anticarcinogenic activity of APG and the promising activity of this active liquid lipid.[26,27]

A dual formulation of last-generation lipid nanoparticles was developed and optimised for administration of APG and rosehip oil. Physicochemical and morphological characterisation, compound interactions, and in vitro release profiles were studied. Moreover, their antiangiogenic properties and cellular internalisation were evaluated. Furthermore, the antiproliferative activity in different tumour cell lines was assesed.

Materials and Methods

Materials

APG was obtained from Apollo Scientific (Cheshire, UK). Compritol® 888 ATO was kindly gifted by Gattefossé (Madrid, Spain). Tween® 80 (polysorbate 80) and Nile Red (NR) were purchased from Sigma–Aldrich (Madrid, Spain). Rosehip oil was purchased from Acofarma Fórmulas Magistrales (Barcelona, Spain). All the other reagents were of analytical grade. A Millipore Milli-Q Plus system was used to obtain purified water.

Preparation of APG-NLC

The production of APG-NLC was carried out using the hot high-pressure homogenisation method (Homogeniser FPG 12800, Stansted, United Kingdom). Firstly, a primary emulsion with a mixture of an aqueous phase containing the surfactant, and a lipid phase containing the lipids and the drug, was prepared using an Ultraturrax® T10 basic (IKA, Germany) at 8.000 rpm for 30 s. The production conditions were 85°C, three homogenisation cycles, and 900 bar of pressure.[28]

The production of APG-NLC labelled with NR (APG-NLC-NR) was carried out following the same procedure as APG-NLC, but with the addition of a 0.0375 % of NR to the formulation.[29]

Optimization of APG-NLC

Design of Experiments (DoE) was used to optimise the formulation parameters because of its ability to acquire information by decreasing the number of experiments.[30,31] A central composite factorial design (which contained 2 replicated centre points, 16 factorial points, and 8 axial points) was prepared using Statgraphics Centurion® 18 version 18.1.12 software (Virginia, USA). Four independent variables, APG concentration, surfactant concentration, lipid phase concentration, and solid lipid concentration (LS/lipid phase), were analyzed to determine their effect on NLC physico-chemical properties. The dependent variables studied were the mean particle size (Z_{av}), polydispersity index (PDI), zeta potential (ZP), and encapsulation efficiency (EE).

Physicochemical Characterization of APG-NLC

Z_{av} and PDI were evaluated by dynamic light scattering by using a ZetaSizer Nano ZS (Malvern Instruments, Malvern, UK). Electrophoretic mobility was used to assess the ZP. For Z_{av} and PDI, the formulations were diluted 1:10 with Milli-Q water. For ZP measurements, the nanoparticles were diluted 1:20. The entrapment efficiency (EE) was indirectly measured by quantifying the non-encapsulated APG in the APG-NLC. Prior to analysis, the non-encapsulated APG was separated from NLC by filtration/centrifugation at 14,000 rpm (Mikro 22 Microliter Centrifuge, Germany) using an Amicon® Ultra-0.5 centrifugal filter device (Amicon Millipore Corporation, Ireland). The non-encapsulated APG passed through the filter, which was analysed by HPLC. EE was determined using Eq. 1:[32]

$$EE\ (\%) = \frac{Total\ initial\ amount\ of\ APG - non - encapsulated\ APG}{Total\ initial\ amount\ of\ APG} \cdot 100 \quad (1)$$

APG quantification was performed using reverse-phase high-performance liquid chromatography (RP-HPLC). In brief, samples were quantified using HPLC Waters 2695 (Waters, Massachusetts, USA) separation module, and a Kromasil® C18 column (5 µm, 150 × 4.6 mm) with a mobile phase formed by a water phase containing 2 % acetic acid, and an organic phase constituted by methanol. A gradient was applied (from 40 % to 60 % of water phase in 5 min and back in next 5 min) at 0.9 mL/min. To quantify APG, a diode array detector Waters® 2996 at 300 nm was used, and data were evaluated using Empower® 3 Software.[33,34]

Interaction Studies

Interaction Studies

Differential scanning calorimetry (DSC) was performed on a DSC 823e system (Mettler-Toledo, Barcelona, Spain). Thermograms of APG-NLC and their components were obtained in a nitrogen atmosphere by using a heating ramp from 25 to 105 °C at 10 °C/min. The data acquired was evaluated with the software Mettler STARe V 9.01 dB (Mettler-Toledo, Barcelona, Spain).[28,32]

Fourier transform infrared (FTIR) spectra of APG-NLC and their components were determined using a Thermo Scientific Nicolet iZ10 spectrometer coupled to a diamond ATR crystal and a DTGS detector (Barcelona, Spain).[35]

X-ray diffraction (XRD) profile of APG-NLC and their components was also assessed placing the samples between two polyester layers of 3.6 µm and exposing them to CuKα radiation (45 kV, 40 mA, λ = 1.5418 Å), in a working range (2θ) of 2–60°, and using a step size of 0.026°, during 200 s per step.[28]

Morphological Studies

Transmission electron microscopy (TEM) was employed to determine the morphology of the APG-NLC using a Jeol 1010 (Jeol USA, Massachusetts, USA). Firstly, copper grids were activated by UV light, and the APG-NLC (previously diluted 1:10) were stained negatively with 2% of uranyl acetate.[32]

Stability Studies

APG-NLC were stored at 3 different temperatures (4, 25, and 37°C) for several months. The study was performed by analysing light backscattering (BS) profiles using Turbiscan® Lab equipment (Formulation Inc, Worthington, USA). For this purpose, 10 mL of the sample was placed into a glass measurement cell, and BS data were acquired every 15–30 days. At the same timepoints, the values of Z_{av}, PDI, ZP, and EE were measured at 15 days or once a month until destabilization.[31]

Biopharmaceutical Behaviour

The in vitro APG release study was carried out by using Franz-type diffusion cells (Permegear, Germany) with a diffusion area of 0.20 cm^2 and cellulose dialysis membrane (MWCO 12 kDa). A receptor medium accomplishing sink conditions was used, which was constituted by a solution of PBS with 5% Tween® 80 and 20% ethanol at pH 7.4.[36] The formulations were compared to free APG. The assay was carried out at 37 ± 0.5 °C for 48 h. 300 µL of each formulation were placed on the donor compartment, and at certain time intervals, 150 µL of the sample was collected

using a syringe, and the withdrawn volume was replaced with the receptor solution. APG content of the receptor medium was analysed using HPLC. Each sample was performed in triplicate, and the cumulative amount of APG was calculated.[28]

Antiangiogenic Capacity

To determine the antiangiogenic effects of APG-NLC, a modified chorioallantoic membrane (CAM) test was used.[37] It was carried out using fertilised chicken eggs incubated at 37 °C and 85 % humidity. A lateral window was opened on the eggshell on the third day of incubation, and after 24 h of stabilization, 40 µL of the sample were inoculated to the CAM. Afterwards, the membrane was sealed and incubated for 48 h. The controls of the experiments were NaCl as a normal angiogenic development and basic fibroblast growth factor (bFGF) as a pro-angiogenic control (20 µL at 10 ng/mL). Once CAM was evaluated, membranes were fixed by adding 4 % paraformaldehyde overnight at 4 °C. Next, membranes were extracted and observed using a binocular loupe. Afterwards, the obtained images were processed, and the density of the vessels in the CAM was automatically measured using ImageJ vessel analysis plugin.

Biological Studies

Cell Lines

Human biphenotypic B myelomonocytic leukaemia MV4-11 and normal breast epithelial MCF-10A cells were acquired from American Type Culture Collection (USA). Human lung carcinoma A549 and breast cancer MCF-7 cells were from the European Collection of Authenticated Cell Cultures (UK). Human breast cancer MDA-MB-468 cells were acquired from the Leibniz Institute, DSMZ-German Collection of Microorganisms and Cell Cultures (Germany). Cells were grown at 37 °C with 5 % CO_2 humidified atmosphere, and media were supplemented with 2 mM l-glutamine (Merck, Germany), 100 units/mL penicillin (Polfa Tarchomin S.A., Poland), and 100 µg/mL streptomycin (Merck, Germany).

MV4-11 and MDA-MB-468 cells were cultured in RPMI 1640 medium (IIET PAS, Poland) with 1.0 mM sodium pyruvate (only MV4-11), 10% (MV4-11), or 20% (MDA-MB-468) fetal bovine serum (FBS) (all from Merck, Germany). A549 cells were cultured in RPMI 1640+Opti-MEM (1:1) (IIET PAS, Poland and Gibco, UK) supplemented with 5% foetal bovine serum (Merck, Germany). The MCF-7 cells were cultured in Eagle's medium and supplemented with insulin and 1% of MEM non-essential amino acids (Merck, Germany). Normal breast epithelial MCF-10A cells were cultured in the HAM'S F-12 medium (Corning), supplemented with 10 % Horse Serum (Gibco), 0.5 µg/mL Hydrocortisone, 20 ng/mL EGFh, 10 µg/mL insulin, and 0.05 mg/mL Cholera Toxin from *Vibrio cholerae* (all from Merck, Germany).

Determination of Antiproliferative Activity

The solutions of APG (1 mg/mL), APG-NLC (1 mg APG/mL) and empty NLC were prepared by APG and NLC in DMSO and water, respectively. Twenty-four hours prior the addition of the tested compounds, the cells were seeded in 96-well plates (Sarstedt, Germany) at a density of 1×10^4 or 0.5×10^4 (A549) cells/well. Antiproliferative capacity was studied after 24 and 72 h of cells exposure to four different concentrations. Cytotoxic effects were examined using MTT (MV4-11) or SRB assays, previously described.[38] The IC_{50} (inhibitory concentration 50 %), which is cytotoxic to 50 % of the cells, was calculated. IC_{50} values were evaluated for each experiment separately using the Prolab-3 system based on Cheburator 0.4 software,[39] and the mean values ± SD are presented in Table 1. Both APG and APG-NLC were assessed in triplicate, and the experiments were repeated up to 5 times.

Determination of Compounds Accumulation in Cells by Flow Cytometry

The APG-NLC were fluorescently labelled with NR to determine their accumulation in cells. Leukemia MV4-11 cells were incubated for 5, 15, and 30 min and 60, 120, and 240 min with APG-NLC-NR (1.675 and 0.335 µg/mL). After incubation, cells were collected and washed with PBS. The mean fluorescence of cells incubated with the tested compounds labelled with NR was analyzed by flow cytometry using a BD LSRFortessa cytometer (BD Bioscience, San Jose, USA). Untreated cells were used as unlabeled controls. The results were analysed using the Flowing software 2 (Cell Imaging Core, Turku Centre for Biotechnology, University of Turku Åbo Akademi University).

Table 1 Design of experiments and characterization of the different formulations developed

Independent Variables								Dependent Variables			
Coded Level	**cApig (%)**	**Coded Level**	**cLipid (%)**	**Coded Level**	**cLS (%)**	**Coded Level**	**cTw (%)**	**Z_{av} ± SD (nm)**	**PDI ± SD**	**ZP ± SD (mV)**	**EE ± SD (%)**
Factorial points											
-1	0.1	-1	5	1	85	-1	2	176.1 ± 2.3	0.278 ± 0.009	-21.7 ± 0.7	99.9 ± 0.1
1	0.2	-1	5	-1	65	1	4	221.5 ± 2.5	0.313 ± 0.012	-21.4 ± 0.5	96.7 ± 0.1
1	0.2	1	10	-1	65	-1	2	253.9 ± 4.4	0.246 ± 0.012	-22.6 ± 0.3	99.9 ± 0.1
-1	0.1	1	10	1	85	-1	2	271.4 ± 5.5	0.273 ± 0.008	-23.0 ± 0.8	99.9 ± 0.1
-1	0.1	1	10	-1	65	-1	2	243.7 ± 0.7	0.236 ± 0.014	-24.6 ± 0.5	99.7 ± 0.3
-1	0.1	1	10	-1	65	1	4	214.7 ± 1.6	0.181 ± 0.010	-18.2 ± 0.9	99.9 ± 0.1
-1	0.1	-1	5	1	85	1	4	165.9 ± 1.2	0.265 ± 0.012	-17.6 ± 0.2	99.9 ± 0.1
-1	0.1	-1	5	-1	65	-1	2	161.2 ± 2.3	0.255 ± 0.023	-22.3 ± 0.4	95.1 ± 0.2
1	0.2	1	10	-1	65	1	4	212.2 ± 1.8	0.217 ± 0.019	-19.6 ± 0.2	99.9 ± 0.1
-1	0.1	1	10	1	85	1	4	236.8 ± 2.0	0.244 ± 0.017	-18.4 ± 0.5	99.9 ± 0.1
1	0.2	-1	5	1	85	1	4	191.9 ± 2.7	0.318 ± 0.058	-19.2 ± 0.6	99.9 ± 0.1
-1	0.1	-1	5	-1	65	1	4	202.7 ± 2.4	0.203 ± 0.002	-18.7 ± 0.2	97.7 ± 0.1
1	0.2	1	10	1	85	-1	2	304.6 ± 5.7	0.276 ± 0.007	-20.1 ± 0.4	99.1 ± 0.1
1	0.2	-1	5	-1	65	-1	2	188.7 ± 2.3	0.374 ± 0.008	-22.2 ± 0.4	99.9 ± 0.1
1	0.2	1	10	1	85	1	4	240.5 ± 2.5	0.277 ± 0.015	-18.0 ± 0.4	99.6 ± 0.1
1	0.2	-1	5	1	85	-1	2	200.5 ± 2.8	0.425 ± 0.015	-22.4 ± 0.6	99.9 ± 0.1
Axial points											
-2	0.05	0	7.5	0	75	0	3	181.2 ± 1.4	0.221 ± 0.029	-19.5 ± 0.3	99.9 ± 0.1
2	0.25	0	7.5	0	75	0	3	230.3 ± 2.7	0.327 ± 0.007	-20.2 ± 0.2	99.9 ± 0.1
0	0.15	-2	2.5	0	75	0	3	202.0 ± 3.9	0.556 ± 0.015	-22.3 ± 0.3	99.9 ± 0.1
0	0.15	2	12.5	0	75	0	3	280.9 ± 5.7	0.259 ± 0.009	-20.7 ± 0.4	99.9 ± 0.1
0	0.15	0	10	-2	55	0	3	187.3 ± 1.3	0.195 ± 0.012	-20.4 ± 0.5	99.9 ± 0.1
0	0.15	0	10	2	95	0	3	202.5 ± 3.3	0.331 ± 0.026	-20.7 ± 0.2	99.9 ± 0.1
0	0.15	0	10	0	75	-2	1	271.0 ± 4.3	0.231 ± 0.020	-24.1 ± 0.7	99.9 ± 0.1
0	0.15	0	10	0	75	2	5	239.1 ± 1.6	0.182 ± 0.027	-17.2 ± 0.8	98.1 ± 0.3
Central points											
0	0.15	0	7.5	0	75	0	3	202.0 ± 0.8	0.267 ± 0.012	-20.3 ± 0.4	99.9 ± 0.1
0	0.15	0	7.5	0	75	0	3	199.3 ± 0.7	0.292 ± 0.038	-19.6 ± 0.1	99.9 ± 0.1

https://doi.org/10.2147/IJN.S429565

Results

APG-NLC Characterization and Optimization

The homogenisation parameters in order to produce NLC by high-pressure homogenization were previously optimised using a composite factorial design with three levels and two factors. The independent variables were pressure, number of homogenisation cycles, and primary emulsion time, and the dependent variables were Z_{av} and PDI (Figure 1). The results showed that with an increase in the number of homogenisation cycles up to two and pressures up to 800 bar, it was possible to produce nanocarriers with lower Z_{av} and PDI. However, it was established that the primary emulsion time using Ultraturrax® did not affect the studied parameters; therefore, the method was set up in three homogenisation cycles at 900 bar with a primary emulsion time of 30 s.

An optimised formulation was obtained by means of the DoE approach. The independent variables studied were the amount of APG, the lipid phase (solid lipid and liquid lipid mixture), the percentage of solid lipids in the lipid phase, and the amount of surfactant.

Table 1 shows the effect of the independent variables on the dependent variables analysed and the values obtained. As can be observed, the Z_{av} of the formulations was 200 nm in most cases, as well as PDI values around 0.2, thus indicating a homogeneous distribution of nanoparticles.[40] The developed APG-NLC exhibited a negative surface charge of ZP < −20 mV. This negative charge may be due to the ionisation of glyceryl behenate (a fatty acid in Compritol® 888 ATO).[41] Since the surface charge values are associated with the stability of colloidal dispersions, the developed formulations with values of −20 mV were considered the most stable.[42] In all cases EE was higher than 95%, thus meaning that APG was completely encapsulated.

As shown in Figure 2, the four variables studied had a significant effect on the formulation of NLC. The Z_{av} and PDI of APG-NLC were significantly influenced by the concentration of the lipid phase but followed an opposite trend because more solid lipids increased size ($p < 0.05$) but decreased NLC PDI ($p < 0.01$). Moreover, the surface charge was significantly influenced by the surfactant ($p < 0.001$), and the EE % was significantly influenced by both liquid and solid lipids.

As shown in Figure 3, higher concentrations of the lipid phase provided larger APG-NLC but with less size dispersion (Figure 3A and B). According to the surface response, in order to obtain APG-NLC below 200 nm, less than 9 % of lipid

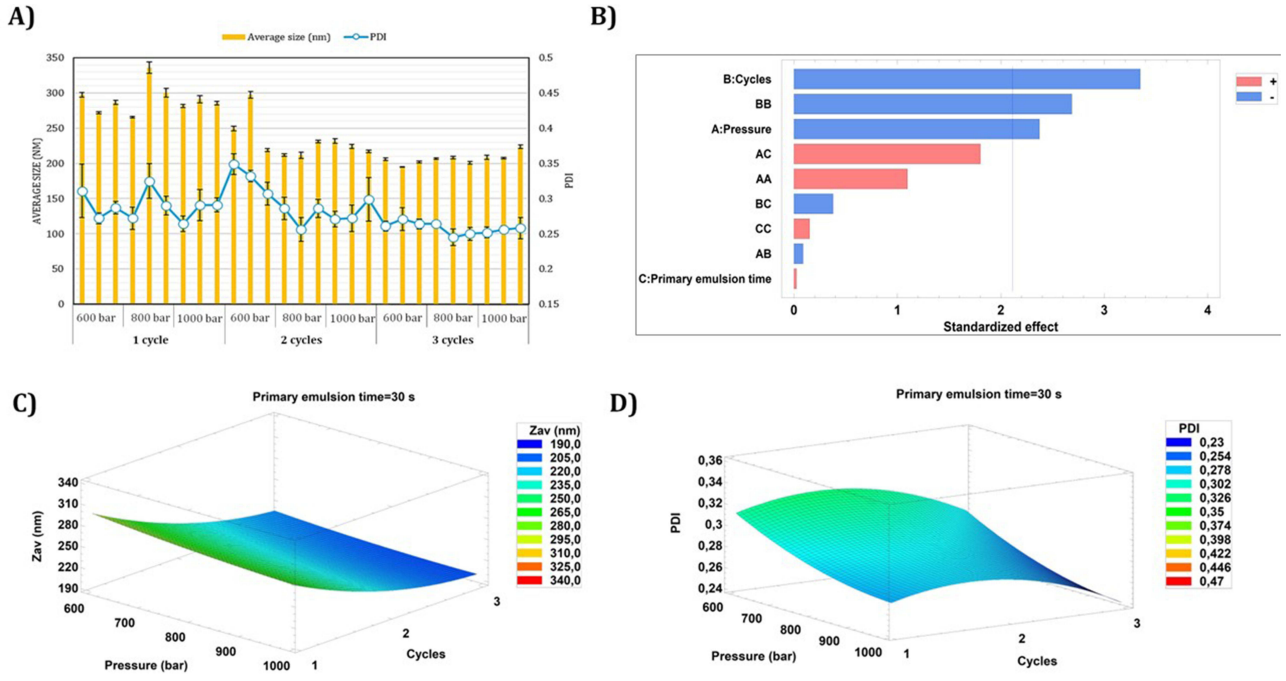

Figure 1 Initial screening for APG-NLC development. (**A**) Representation of the values obtained of Z_{av} and PDI against the homogenization cycles and homogenization pressure; (**B**) Pareto's chart of the homogenization parameters; (**C**) Surface response of the influence of the pressure and cycles on the Zav; (**D**) Surface response of the influence of the pressure and cycles on the PDI.

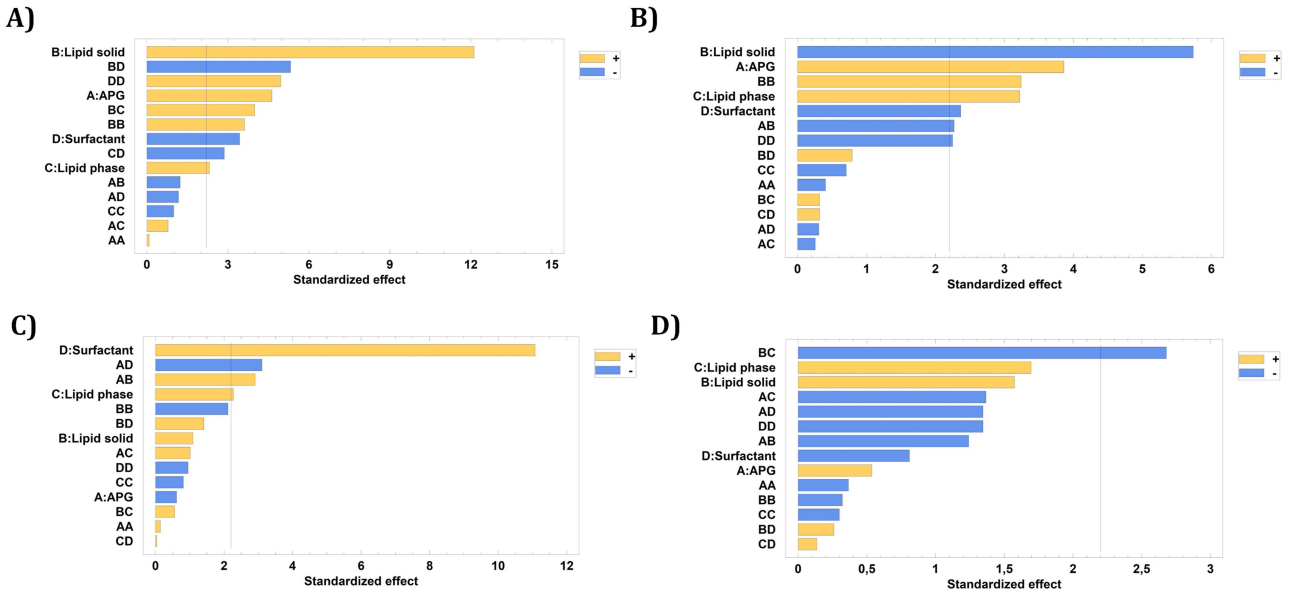

Figure 2 Pareto's chart of the influence of the independent variables for each dependent variable. (**A**) Z_{av}; (**B**) PDI; (**C**) ZP; (**D**) EE.

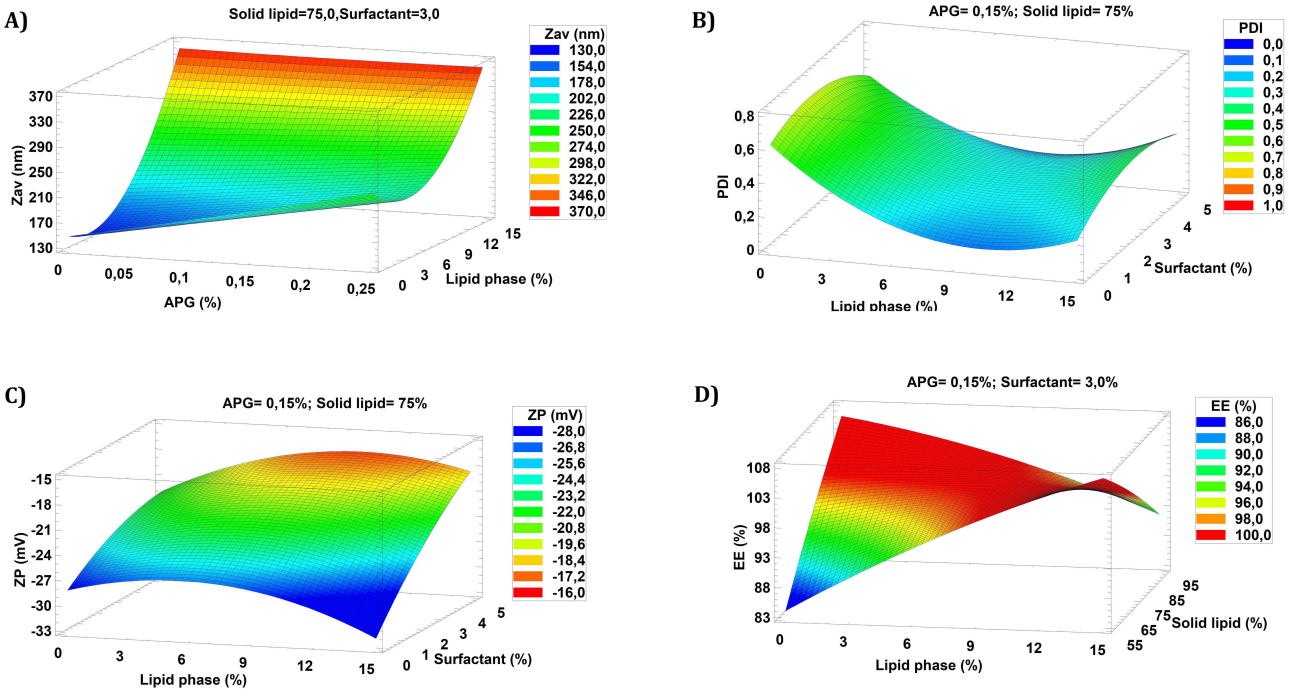

Figure 3 DoE surface response of APG-NLC. (**A**) Concentration of Solid lipid regarding to the lipid phase and Surfactant influence on Z_{av}; (**B**) Concentration of APG and Solid lipid regarding to the lipid phase influence on PDI; (**C**) Concentration of Surfactant and Solid lipid regarding to the lipid phase influence on ZP; (**D**) Concentration of APG and Surfactant influence on EE.

phase and APG concentrations below 0.2 % should be used. However, to obtain a PDI of less than 0.2, higher concentrations of the lipid phase seem necessary. Moreover, with respect to ZP, a lower surface charge was obtained when a higher concentration of the surfactant was added (Figure 3C). EE was highly influenced by the amount of solid lipids with low EE as the solid lipid content increased (Figure 3D). Considering all the evaluated parameters and the trends, a formulation containing 0.1 % of APG, 7.5 % of total lipids, 65 % of solid lipids, and 3.5 % of surfactant has been optimized to carry out further experiments.

Interaction Studies of APG-NLC

The interactions between APG and the lipid matrix, carried out by DSC, FTIR, and XRD are shown in Figure 4. DSC was performed to study the variations in the crystallinity and melting point of the lipid mixtures against APG-NLC. In this sense, the melting temperature (T_m) of the lipid mixture was slightly lower than that of the lipid mixture with APG (69.50 and 70.22°C, respectively). Moreover, the T_m of the APG-NLC was slightly lower than that of the physical mixture, probably because of its small size and surfactant incorporation.[43] Enthalpy values (ΔH) were similar between the lipid mixture and lipid mixture-APG (ΔH Lipid mixture = 88.87 Jg^{-1}, ΔH Lipid mixture-APG = 97.79 Jg^{-1}). Moreover, ΔH of APG-NLC was lower being 71.10 Jg^{-1}. In addition, APG was also assessed showing a T_m of 365.5°C and ΔH = 198.5 Jg^{-1}.[44]

FTIR analysis was used to study the interactions between APG, surfactant, and the lipid matrix (Figure 4B). The FTIR spectrum of pure APG presented vibrational bands at approximately 3278 cm^{-1}, characteristic of the O-H group. Moreover, the C-H group exhibits multiple small peaks at 2800 cm^{-1}. Additional peaks at 1650 and 1605 cm^{-1} were observed for the C-O group.[45] Furthermore, there was no evidence of new strong bonds formed in the APG-NLC, and APG peaks were not observed, thus confirming APG encapsulation in the lipid matrix.

The XRD profiles in Figure 4C show the physical states of the APG, APG-NLC, and their physical mixture. Intense and sharp peaks for APG and the solid mixture of lipids are observed, indicating that these components possess a crystalline structure. Typical signals of APG such as 7.07, 10.09, 11.25, 14.12, 15.03, 15.97, and 18.18° (2θ) were found.[46] Interestingly, APG peaks were not detected in the APG-NLC, which may indicate that APG was present in a dissolved state in the NLC (molecular dispersion). Additionally, the crystallinity of the structures of all components was studied. The lipid mixture showed three peaks, the smaller one in 19.34° (2θ), ie d = 0.46 nm, indicated the most stable form of triacylglycerols, the β form, and two pronounced peaks at 21.38° (2θ) ie d=0.42 nm and 23.43° (2θ) ie d=0.38 nm, indicating the second stable form of triacylglycerols, the β' form. In contrast, the APG-NLC profile showed the most intense peak at 19.39° (2θ) and 23.62° (2θ), indicating good stability of the formulation.[44,47,48]

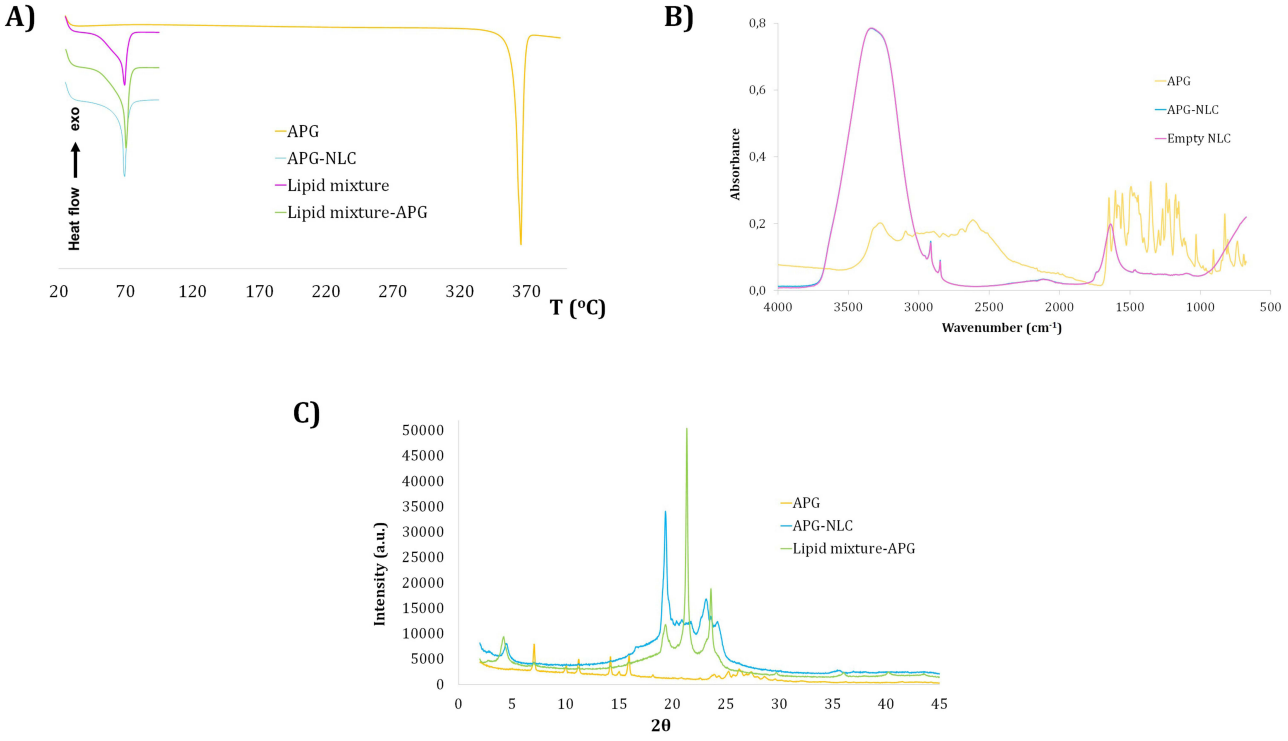

Figure 4 Interaction studies of APG-NLC and their components. (**A**) DSC curves; (**B**) FTIR analysis; (**C**) X-ray diffraction patterns.

Morphological Studies

Due to the fact that a single technique is not enough to characterise NLC, the morphology of the APG-NLC was evaluated by TEM and compared with the results obtained by dynamic light scattering (Figure 5). Using TEM, it can be observed that the APG-NLC showed almost spherical and soft round shapes with Z_{av} values below 200 nm. This was consistent with the results found by dynamic light scattering. Moreover, as predicted by the obtained ZP values (−20 mV), particle aggregation was not observed.

Stability of APG-NLC

Stability studies were performed by measuring Z_{av}, PDI, ZP, and EE as well as by analysing the BS profiles at different temperatures. Specifically, BS provides information on destabilisation mechanisms, such as sedimentation, agglomeration, or aggregation, which can be observed when differences greater than 10 % are obtained.[49] In this way, BS profiles of APG-NLC were studied at 4, 25, and 37 °C (Figure 6). The APG-NLC formulation was stable at 4 °C for a period of 11 months, maintaining constant physicochemical parameters, while at 25 °C, the stability endured 3 months, and at 37°C, it was stable for only 15 days.

Moreover, high temperatures accelerated particle destabilisation by decreasing the ZP. As it can be seen in Table 2, the formulations kept at three different temperatures maintained their physicochemical parameters until the ZP diminished (12 months at 4 °C, 4 months at 25 °C and 15 days at 37 °C). All these phenomena were in accordance with the BS results. As can be observed, at all the temperatures, the BS profile increased, probably because of decrease in ZP, promoting aggregation phenomena that, in the case of 4 °C, seem to start after 1 year of storage. Additionally, the EE was maintained at all temperatures. Considering these results into account, APG-NLC were stored at 4°C showing a good stability up to 12 months.

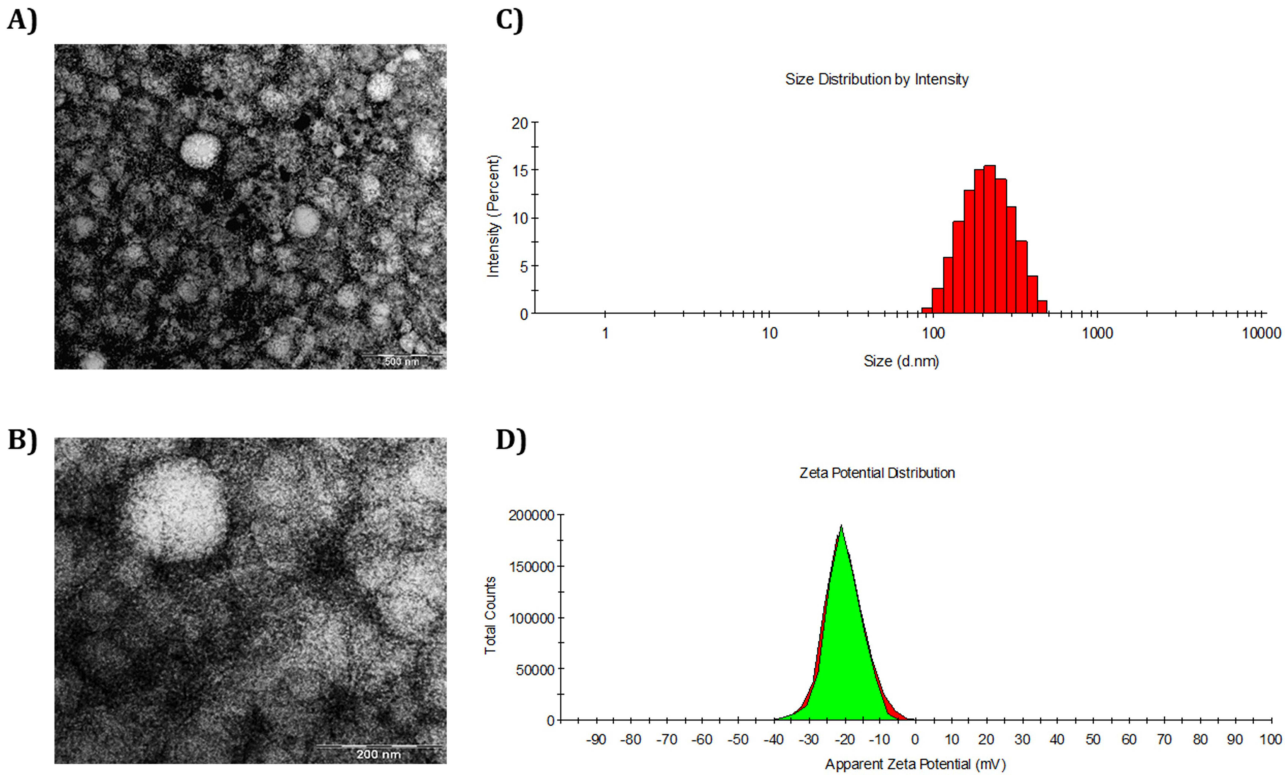

Figure 5 Physicochemical and morphological characterization. (**A**) TEM images with scale bar 500 nm; (**B**) TEM images with scale bar 200 nm; (**C**) Histogram of average size distribution measured by dynamic light scattering; (**D**) Zeta potential plot measured by laser-Doppler electrophoresis.

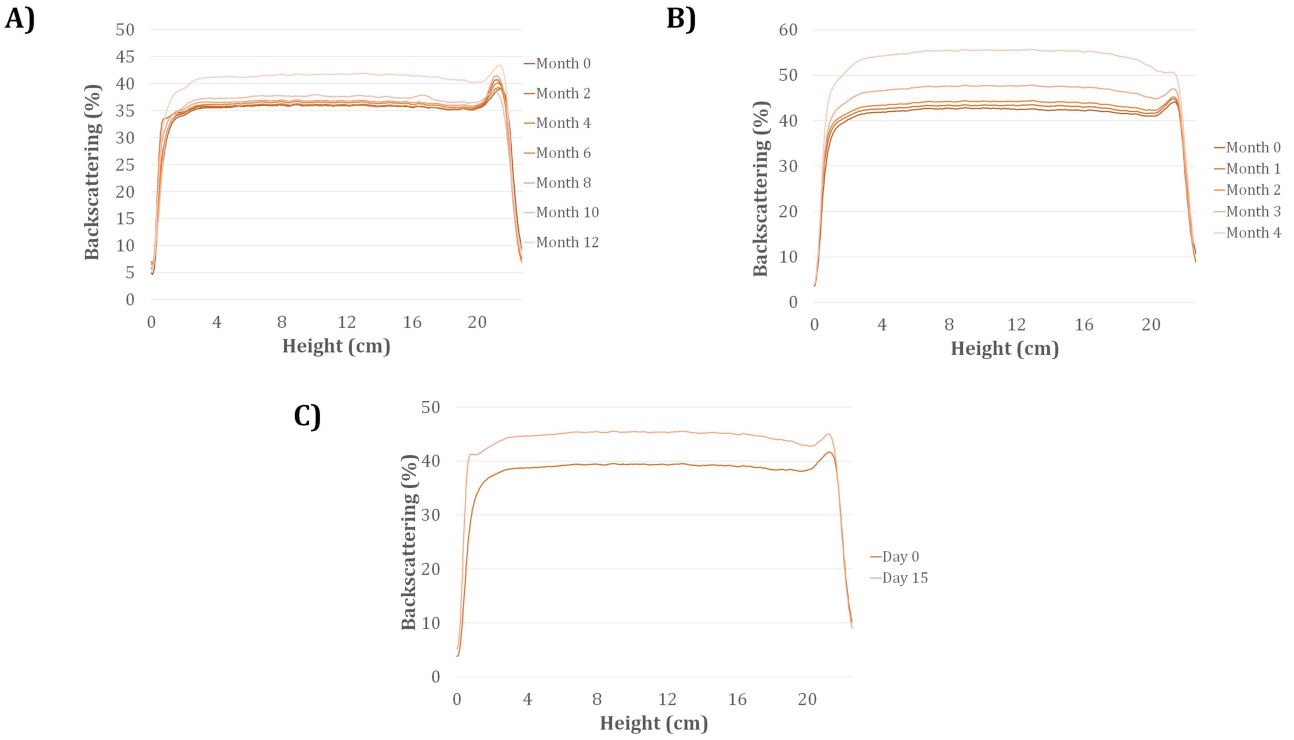

Figure 6 Backscattering profiles of APG-NLC stored at (**A**) 4 °C; (**B**) 25 °C; and (**C**) 37 °C.

Biopharmaceutical Behaviour

The in vitro release profile of APG from NLC against free APG demonstrated that the lipid formulation had a kinetic profile characteristic of prolonged drug release formulations. The APG release from NLC best fit was a two-phase association. As shown in Figure 7, an initial burst release of APG from the NLC was observed during the first 2 h. Afterwards, a slow release of APG occurs probably releasing the APG encapsulated in the inner lipid core. Moreover, free APG showed a fast release, achieving a 100 % before 24 h while the APG-NLC just released less than 30 %. The dissociation constant (K_d) of APG-NLC was higher in both the slow and fast phases than in free APG (0.07 and 0.27 vs 0.02 h), thus indicating a prolonged release.[37] Moreover, the half-life results ($t_{1/2}$) showed that there was a burst release at the beginning during the fast phase of the formulation, but during the slow phase, it had a sustained release, with a $t_{1/2}$ value of 160.5 h.[50]

Table 2 Physicochemical Parameters of APG-NLC Stored at Different Temperatures

Temperature (°C)	Month/Day	Z_{av} ± SD (nm)	PDI ± SD	ZP ± SD (mV)	EE ± SD (%)
	0	195.2 ± 0.4	0.170 ± 0.011	−19.3 ± 0.1	99.9 ± 0.1
4	2	193.2 ± 0.7	0.171 ± 0.026	−17.7 ± 0.3	99.9 ± 0.1
	4	195.4 ± 0.9	0.160 ± 0.002	−17.0 ± 0.3	99.9 ± 0.1
	6	194.9 ± 0.3	0.164 ± 0.017	−17.7 ± 0.2	99.9 ± 0.1
	8	195.0 ± 1.8	0.148 ± 0.009	−17.5 ± 0.4	99.9 ± 0.1
	10	193.0 ± 1.9	0.151 ± 0.015	−20.8 ± 0.3	99.9 ± 0.1
	12	193.5 ± 2.1	0.161 ± 0.002	−15.2 ± 0.2	99.9 ± 0.1
25	2	201.9 ± 2.9	0.123 ± 0.017	−18.3 ± 0.2	99.9 ± 0.1
	4	199.8 ± 1.7	0.125 ± 0.034	−14.8 ± 0.3	99.9 ± 0.1
37	15 days	209.2 ± 0.9	0.161 ± 0.025	−15.5 ± 0.3	99.9 ± 0.1

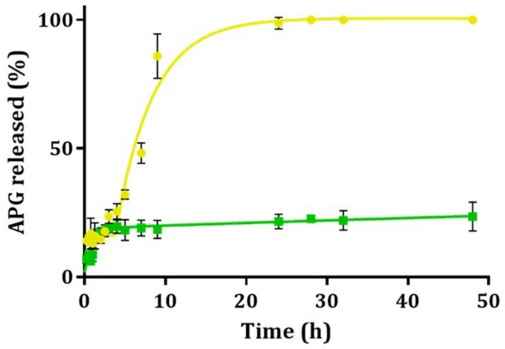

Parameter	Free APG	APG-NLC
K_d (h)	0.02298	K_{fast} = 0.2662 K_{slow} = 0.06623
$t_{1/2}$ (h)	3.18	$t_{1/2\ fast}$ = 0.7728 $t_{1/2\ slow}$ = 160.5
R^2	0.7745	0.9765

Figure 7 In vitro release profile of APG-NLC vs free APG carried out for 48 h and adjustment to a two-phase association and Plateau followed by one phase decay model respectively.

Antiangiogenic Capacity

To study the antiangiogenic capacity of free APG, APG-NLC, and empty NLC, an in vitro assessment using CAM of embryonated eggs was carried out. As shown in Figure 8, APG-NLC possessed a significantly lower ($p < 0.01$) vascular density than the negative control (NaCl). Although free APG seems to exert antiangiogenic effects, these effects are not significant. Moreover, empty NLC did not seem to have any effect on the blood vasculature.

Cytotoxicity Towards Selected Cancer Cell Lines

The antiproliferative activities of APG and APG-NLC towards leukemia (MV4-11), lung (A549), and two breast MCF-7 (ER+) and MDA-MB-468 cancer cell lines were evaluated after 24 h and 72 h. The toxicity of these compounds was tested in normal human breast epithelial MCF-10A cells. The results were obtained by assessing cellular viability using MTT (MV4-11) or SRB colorimetric assays. The data for the in vitro anticancer activity are reported in Table 3 and expressed as the IC_{50} concentration of the compound (in μg/mL) that inhibited proliferation of the cells by 50% compared to the untreated control cells.

As shown in Table 3, APG after 24 h of incubation was active only against leukaemia MV4-11 cells, and the activity was 10 times lower than that observed after 72 h. Both empty and APG-NLC had similar activity after 24 h and 72 h against MV4-11 leukemia cells, whereas in human lung cancer A549 cells, the activity was similar only after 72

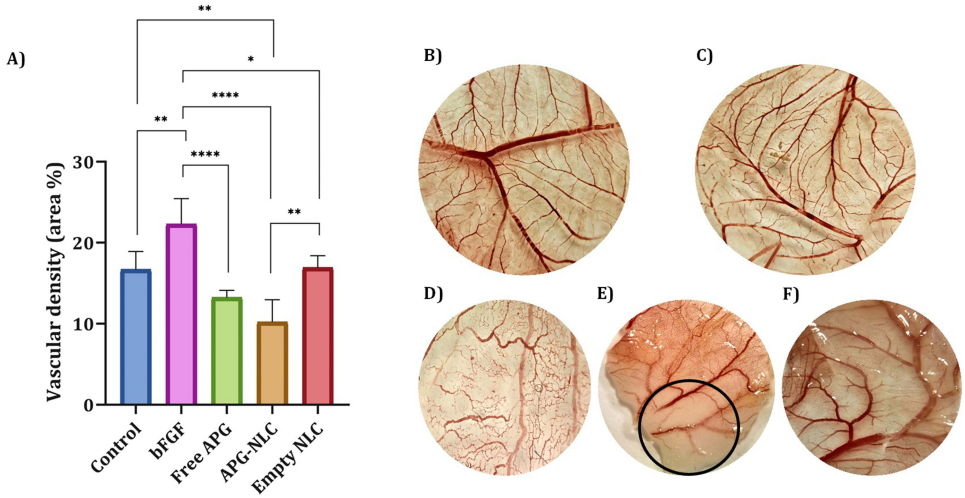

Figure 8 Anti-angiogenic capacity. (**A**) Measurement of the vascular area (%) of the extracted membranes after 48 h of stimulation with each compound. Differences between groups analysed by one-way ANOVA; (* $p < 0.05$; ** $p < 0.01$; ****$p < 0.001$); (**B–F**) Membranes after the incorporation of 48 h of product: (**B**) bFGF, (**C**) NaCl, (**D**) Free APG, (**E**) APG-NLC with a black circle highlighting its effect, (**F**) Empty NLC.

Table 3 The Half Maximal Inhibitory Concentrations (IC_{50}) of APG, Empty NLC and APG-NLC Against Selected Cancer Cell Lines and Non-Tumorigenic Human Breast Epithelial Cell Line (MCF-10A)

Compound	Cell Lines IC_{50} [μg/mL]									
	MV4-11		A549		MDA-MB-468		MCF-7		MCF-10A	
	24h	72h	24h	72h	24h	72h	24h	72h	24h	72h
APG	23.0 ± 9.8	2.5 ± 0.7	n.a.	33.5 ± 6.3	n.a.	11.3± 2.6	n.a	26.0 ± 5.9	n.a	10.1 ± 5.0
Empty NLC	0.4 ± 0.0	0.5 ± 0.2	2.3 ± 0.4	2.6 ± 0.7	2.5 ± 0.5	0.6 ± 0.2	16.4 ± 1.3	2.3 ± 0.3	n.a	20.5 ± 4.8
APG-NLC	0.3 ± 0.1	0.3 ± 0.1	7.7 ± 3.2	2.4 ± 0.3	2.9 ± 0.9	0.4 ± 0.1	16.2 ± 0.6	1.8 ± 0.6	n.a	14.9 ± 5.6

Notes: n.a. – not active, IC_{50} value higher than 33.5 μg/mL. Data are presented as mean ± standard deviation (SD) calculated using Prolab-3 system based on Cheburator 0.4 software.

h. Probably due to slow APG release, after 24 h, the activity was lower in the case of APG-NLC. Additionally, in breast cancer cells, the effect was more potent after 72 h of incubation.

Moreover, the IC_{50} of the APG-NLC was 10–27 times lower against cancer cells than that of free APG. According to the results obtained in Table 3, the most sensitive cell lines were leukemia MV4-11 and breast cancer MDA-MB-468 cells. Moreover, the comparison of APG-NLC anticancer activity against two different breast cancer models showed that APG-NLC after 24 h and 72 h was more active against triple negative breast cancer (TNBC) MDA-MB-468 cells (IC_{50} 2.9 μg/mL and 0.41 μg/mL) than ER-positive MCF-7 cells (IC_{50} 16.2 μg/mL and 1.8 μg/mL). TNBC is usually more aggressive, harder to treat, and more likely to come back (recur) than cancers that are hormone receptor- or HER2-positive. APG-NLC also showed selective efficacy against tumour cells compared with normal MCF-10A cells (SI index >1, Table 4). Importantly, this selectivity was not observed for the free APG, because it showed cytotoxicity in both, the healthy and the cancer cell line.

Accumulation of APG-NLC in Tumoral Cells

To determine whether APG nanoformulations have the ability to accumulate in leukemia cells, a cytometric method and staining of cell culture with the fluorescent dye NR was proposed. This dye binds to neutral fats and phospholipids. The amount of bound dye is directly proportional to the content of neutral fats in the cells. Leukemia cells MV4-11 were incubated with fluorescently labelled formulation APG-NLC-NR (two concentrations of APG-NLC-NR were studied, 0.335 and 1.675 μg/mL, respectively). After several time points, cell fluorescence was analysed using flow cytometry, and the results are presented in Figure 9A and B. The obtained results confirm the assumption of the conducted research that NLC formulations are an effective method of delivering biologically active substances inside the cells. The mean fluorescence intensity (MFI) of the cells after incubation with APG-NLC-NR was compared with that of the control (unlabelled cells). As shown in Figure 9A, after 5 min of incubation with labelled APG-NLC-NR, significantly higher fluorescence was observed. At all time points, a significantly higher MFI was obtained than that of the control ($p < 0.05$). Moreover, the accumulation of APG-NLC in the cells was fast and stable, and after 5 min, significant differences against the control were obtained. After 240 min of incubation, the MFI values were maintained. The confirmation of accumulation of APG-NLC-NR in the cancer cells is also the graph Figure 9B on which histogram for cells incubated

Table 4 The Selectivity Index (SI) of Tested Compounds

Compound	Cell Lines/Calculated Selectivity Index SI			
	MV4-11	A549	MDA-MB-468	MCF-7
APG	4.04	0.31	0.89	0.39
Empty NLC	41.00	7.88	34.17	8.90
APG-NLC	55.20	6.30	36.30	8.30

Notes: The SI index = IC_{50} for normal cell line (MCF-10A)/ IC_{50} for respective cancerous cell line. A beneficial SI > 1.0 indicates a drug with efficacy against tumor cells greater than toxicity against normal cells.

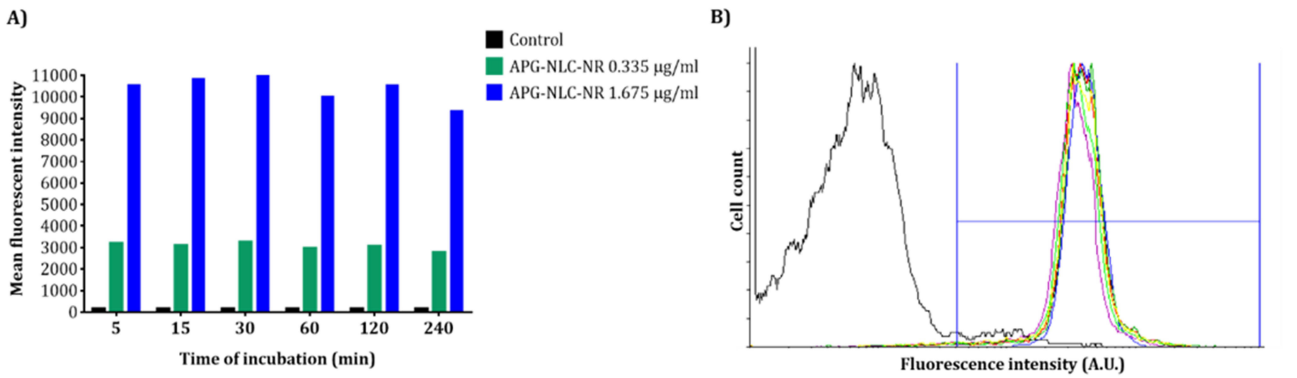

Figure 9 Accumulation of APG-NLC in MV4-11 cells. (**A**) Mean fluorescent intensity after 5, 15, 30, 60, 120, 240 min with low and high concentration of APG-NLC; (**B**) Flow cytometry histogram for higher concentration (1.675 µg/mL) of APG-NLC-NR. Black line: unlabelled control, red line: after 5 min; dark green line: after 15 min; blue line: after 30 min, light green line: after 60 min; yellow line: after 120 min and purple line: after 240 min.

with labelled formulations is shifted in higher fluorescence intensity (A.U.) in comparison to control free unlabelled leukaemia cells.

Discussion

In this study, a new formulation was developed loading of APG into a rosehip-based NLC. The fabrication method selected was hot high-pressure homogenization, due to its multiple advantages such as its ability of large-scale production, the avoidance of organic solvents, and its low cost.[51] Due to the high energy input, it allows to prepare small uniform particles, which is suitable for nanoparticulate formulations.[52]

To optimise the formulation, a design of experiments was applied. Using these studies, a full factorial design was developed, and the analysis showed that all parameters induced statistically significant differences in Z_{av}, in which the concentration of the lipid phase had the greatest influence, followed by the concentration of APG. These results are in accordance with those obtained by other authors, in which increased drug and lipid amounts led to larger nanoparticles.[53] Furthermore, the lipid phase significantly influenced the PDI, showing high values when the lipid phase decreased. Otherwise, ZP was mainly affected by the concentration of the non-ionic surfactant Tween® 80, which became more neutral with increasing surfactant amounts. This trend may be related to the absorption of the surfactant onto the NLC surface.[54] Furthermore, APG encapsulation was high in all the assessments (>95%), probably because of the lipophilic character of APG which had more affinity for the lipid-based internal structure of the NLC.[55,56] Other authors encapsulated APG into different NLC matrix by using a hot homogenizer method along with ultrasonication, obtaining smaller nanoparticles, but less stable due to its ZP closer to 0 mV.[57] Other research group prepared SLN encapsulating APG by the melt emulsification and ultra-sonication method, in which they obtained small particles around 100 nm, but with a higher PDI.[58] Moreover, Liang and colleagues also prepared NLC but encapsulating a similar molecule, quercetin, another natural flavone. In their study, they used a low energy method for the preparation of the NLC, the emulsifying technique, leading to a polydisperse formulation (PDI > 0.3).[59]

Interaction studies showed that the lipid matrix of the formulation became more amorphous in the presence of APG, indicating that APG was solubilised in lipids.[60] FTIR studies confirmed that no covalent bonds were formed between the drug and the lipid matrix, so hydrogen bonds and hydrophobic forces could be the main forces between them, facilitating the accommodation of APG inside the NLC and promoting its liberation from the particle.[61] Furthermore, the XRD results suggested that APG-NLC could possess good and long stability due to the presence of the most stable forms of triacylglycerols, the β and β' forms.[44,47,48] These results are in agreement with the stability studies, in which the formulation was stable at 4°C for 12 months. Subsequently, the electrostatic forces between the APG-NLC may begin to decrease, leading to aggregation and sedimentation (as observed in the backscattering profile).[62] Despite this, in some cases, sedimentation can be reversed by agitation, and in order to obtain stability for more than 12 months, APG-NLC

can be freeze-dried.[63] Moreover, interaction studies showed that APG was encapsulated into the NLCdue to the absence of signals of APG in the different studied techniques.

In addition, the APG-NLC showed a sustained in vitro release profile, whereas the APG solution was released rapidly. The fitted model for APG-NLC was a two-phase association, due to the formulation being able to provide a first fast release, followed by a slow and prolonged liberation of APG to the medium. This kind of model explains many chemical and biological processes, which could indicate a more complicated binding kinetics mechanism.[64–66] It was observed that the release of the APG from the NLC reached approximately 30%, showing an initial burst release of APG in the early phase, followed by a delayed release of APG (up to 24 h). Compared to other studies, these NLC showed a slower release, which might be related to the high solubility of APG in the lipid matrix.[67–69]

In in ovo angiogenesis studies, the anti-angiogenic activity of the APG-NLC was confirmed. It is well known that APG exhibits antiangiogenic activity, which is related to its antitumoral properties.[70] The controls of this study were the negative control (NaCl) and a positive growth control (bFGF), which is known to activate angiogenesis. Although bFGF is one of the most effective inducers of angiogenesis, it frequently contributes to pathological angiogenesis by stimulating vascular endothelial mitogenesis and has been frequently used as an angiogenic polypeptide.[71] In this study, a solution of APG at the same concentration as APG-NLC was used (1 mg/mL). The results showed that APG slightly decreased the number of microvessels in CAM. Other authors have reported that at higher concentrations than those assessed (from 1.35 to 5.4 mg/mL), APG was able to suppress normal angiogenesis in chick embryo.[72] In contrast, APG-NLC significantly decreased vascular density in the negative and positive controls. These results indicate that the encapsulation of APG into lipid nanoparticles increases the bioavailability and bioactivity of the flavonoid.[73] Since APG is an inhibitor of several growth factors such as vascular endothelial growth factor (VEGF) and bFGF[74] and empty NLC do not exert any angiogenesis modulation effect, the developed NLC were able to enhance APG penetration, thus enhancing APG antiangiogenic activity.[75–77] Moreover, since angiogenesis provides an expanding tumour with oxygen and nutrients, which are necessary for tumour growth, inhibition of angiogenesis could provide an effective tool for anticancer therapy.[78]

The antiproliferative activity of APG, empty NLC, and APG-NLC towards five different cell lines was evaluated after 24 and 72 h. For the leukaemia cell line (MV4-11), a solution of APG showed greater activity at 72 h than at 24 h. It has been described that APG stimulates signalling pathways that result in cell proliferation inhibition and cell-cycle arrest in fast-cycling cell. Moreover, other authors have confirmed that by increasing the incubation time of APG with leukaemia cells, cytotoxicity increased.[79] APG-NLC showed 20 times more activity than free APG at 24 and 72 h of exposure. This was probably due to the ability of NLC to penetrate into the cells, increasing the amount of drug intracellularly.[80] This was confirmed by flow cytometry, which showed high and fast NLC internalisation. Moreover, in the lung cancer cell line (A549), APG was not active at 24 h, but its activity increased at 72 h. Conversely, APG-NLC showed a greater effect against this cell line, with the highest effect observed at 72 h. The worst prognosis for survival and most treatment-related issues are associated with TNBC, which accounts for 10% to 22% of all cases of breast cancer that are diagnosed. Furthermore, the absence of response to conventional hormonal therapy or therapies directed at specific receptors makes treatment difficult.[81] In order to evaluate the potential of APG in aggressive cancer, the cell line MDA-MB-468 was used. In the first 24 h, the flavonoid solution was not cytotoxic, as reported.[82] At 72 h, it showed higher activity, which could be related to its mechanism of action, targeting different signal transduction pathways.[83] Nevertheless, APG-NLC showed great cytotoxicity against the TNBC cell line after 24 and 72 h. Another breast cancer cell line (MCF-7) showed cytotoxicity similar to that of APG. Other studies have reported that APG inhibits growth and induces apoptosis in a dose-dependent relationship.[84] Similarly, APG-NLC were more cytotoxic than APG, and their activity increased at 72 h, probably because of the sustained release of APG from the formulation. To confirm the safety and selectivity of the tested compounds, the cytotoxicity of the formulations was tested against a non-tumourigenic cell line (MCF-10A), and the SI was calculated. The SI is an important parameter for the development of novel formulations. A low selectivity of compounds means that patients are unable to receive the drug doses necessary to eradicate all cancer cells, because doing so would be fatal and eradicate all other body cells.[85] The results showed that APG was not selective for cancer lines, except for leukaemia cells, whereas APG-NLC were selective for all tumour cells.

In contrast, empty NLC showed similar antiproliferative activity against all tumour cell lines and high selectivity, demonstrating excellent safety and efficacy. Since two of the three ingredients of the empty formulation had described pharmacological interest, this led to the potent antitumour effects of the empty NLC. On the one hand, the non-ionic surfactant Tween 80® can effectively inhibit P-gp and plays an important role in mediating the opening of tight junctions, which could enhance the paracellular uptake of NLC, increasing their permeability.[86,87] On the other hand, besides the traditional medicinal of rosehip oil when applied on the skin, in the last few year researchers have been reporting novel pharmacological features. Rosehip oil is made from the seed of *Rosa canina* sp. and is rich in polyunsaturated fatty acids, linoleic acid, linolenic acid, and phytosterols such as β-sitosterol.[88] Recently, some authors assessed the extract of rosehip against different cancer cell lines, including colon, lung, prostate, cervix, liver, brain, and breast, suggesting its potential role in chemotherapy.[25,89] After treating these cancer cell lines with whole rose hip extract or purified fractions of its most important components, all studies have reported a noticeable decline in cell viability. These antioxidant properties may be responsible for their antiproliferative effect.[25] However, its activity may not only be due to its antioxidant properties but is also capable of preventing cell proliferation.[90] In another study, researchers tested the rosehip extract against TNBC, and the results showed that it was able to decrease cell migration and inhibit cell growth by reducing two enzymes (MAPK and Akt). In addition, in combination with commonly used chemotherapy, it was able to reduce cell proliferation and migration in tissue cultures, suggesting that rosehip extract might be a useful addition to the thorough treatment regime for patients with TNBC.[91] These results revealed that the proposed combination of APG loading of NLC containing rosehip oil could be a promising platform for the treatment of several cancers.

The cellular uptake of APG-NLC was studied by encapsulating the fluorescent dye NR using flow cytometry. The selected cell line was leukaemic owing to its high cytotoxic activity. APG-NLC-NR showed rapid uptake in the first 5 min, and the fluorescence intensity remained stable for all experiments (4 h). These results could explain the high activity against these cells, in which NLC were able to penetrate and remain inside. Some researchers concede that NLC represent a good delivery system owing to their composition. As liquid lipids give NLC a less ordered lipid matrix, drugs may be more effectively accommodated; in this case, the fluorescent die NR prevents premature drug release and fluorescence signal loss. The incorporation of liquid lipids promotes higher cellular uptake and permeability across the cellular membrane.[92,93]

Conclusion

APG was successfully encapsulated into NLC containing rosehip oil with a particle size below 200 nm, a monodisperse population, and high entrapment efficiency. The APG-NLC showed suitable stability for almost one year, as well as prolonged release. In ovo and in vitro assays in tumour cells confirmed that APG increased its activity when encapsulated in NLC. APG-NLC decreased the formation of new blood vessels, highlighting their antiangiogenic activity. Moreover, the antiproliferative assays confirmed APG-NLC selectivity against tumour cells and cytotoxicity in leukaemia, lung, and breast cancer cells. In addition, empty NLC did not show significant antiangiogenic properties, but in vitro antitumoral assessments showed selective cytotoxicity against cancer cells, probably owing to the pharmaceutical properties of rosehip oil.

These findings constitute a first approach for this type of nanoparticles including two natural active ingredients, such as APG and rosehip oil, in which both the encapsulated compound and the matrix contribute to the pharmacological effect, acting in a synergic way. This kind of formulation could establish a novel therapeutic approach for the treatment of cancer.

In conclusion, APG-NLC have been successfully developed and physicochemically characterised, showing prolonged release, antiangiogenic properties, and suitable activity against tumour cell lines.

Acknowledgments

This research was supported by the Spanish Ministry of Science and Innovation (PID2021-122187NB-C32) and by Wrocław University of Environmental and Life Sciences (Poland) under the Leading Research Groups support project. The APC/BPCis were financed/co-financed by Wrocław University of Environmental and Life Sciences.

EBS acknowledges FCT—Fundação para a Ciência e a Tecnologia, I.P., in the scope of the project UIDP/04378/2020 and UIDB/04378/2020 of the Research Unit on Applied Molecular Biosciences—UCIBIO and the project LA/P/0140/2020 of the Associate Laboratory Institute for Health and Bioeconomy—i4HB.

E.S.-L. acknowledges the support of Grants for the Requalification of the Spanish University System.

Disclosure

The authors report no conflicts of interest in this work.

References

1. Ferlay J, Colombet M, Soerjomataram I, et al. Cancer statistics for the year 2020: an overview. *Int J Cancer*. 2021;149(4):778–789. doi:10.1002/IJC.33588
2. Sung H, Ferlay J, Siegel RL, Laversanne M, Jemal ISA, Bray F. Global cancer statistics 2020: GLOBOCAN estimates of incidence and mortality worldwide for 36 cancers in 185 countries. *CA Cancer J Clin*. 2021;71(3):209–249. doi:10.3322/CAAC.21660
3. Gavas S, Quazi S, Karpiński TM. Nanoparticles for cancer therapy: current progress and challenges. *Nanoscale Res Lett*. 2021;16(1):1–21. doi:10.1186/S11671-021-03628-6
4. Yu Z, Gao L, Chen K, et al. Nanoparticles: a new approach to upgrade cancer diagnosis and treatment. *Nanoscale Res Lett*. 2021;16(1):1–17. doi:10.1186/S11671-021-03489-Z
5. Sharma A, Ghani A, Sak K, et al. Probing into therapeutic anti-cancer potential of apigenin: recent trends and future directions. *Recent Pat Inflamm Allergy Drug Discov*. 2019;13(2):124–133. doi:10.2174/1872213X13666190816160240
6. Allahyari M, Motavalizadeh-Kakhky AR, Mehrzad J, Zhiani R, Chamani J. Cellulose nanocrystals derived from chicory plant: an un-competitive inhibitor of aromatase in breast cancer cells via PI3K/AKT/mTOP signalling pathway. *J Biomol Struct Dyn*. 2023;20:1–15. doi:10.1080/07391102.2023.2226751
7. Taheri R, Hamzkanlu N, Rezvani Y, et al. Exploring the HSA/DNA/lung cancer cells binding behavior of p-Synephrine, a naturally occurring phenyl ethanol amine with anti-adipogenic activity: multi spectroscopic, molecular dynamic and cellular approaches. *J Mol Liq*. 2022;368:120826. doi:10.1016/J.MOLLIQ.2022.120826
8. Kalhori F, Yazdyani H, Khademorezaeian F, et al. Enzyme activity inhibition properties of new cellulose nanocrystals from Citrus medica L. pericarp: a perspective of cholesterol lowering. *Luminescence*. 2022;37(11):1836–1845. doi:10.1002/BIO.4360
9. Ahmed SA, Parama D, Daimari E, et al. Rationalizing the therapeutic potential of apigenin against cancer. *Life Sci*. 2021;267:118814. doi:10.1016/J.LFS.2020.118814
10. Malek-Esfandiari Z, Rezvani-Noghani A, Sohrabi T, Mokaberi P, Amiri-Tehranizadeh Z, Chamani J. Molecular dynamics and multi-spectroscopic of the interaction behavior between bladder cancer cells and calf thymus DNA with rebeccamycin: apoptosis through the down regulation of PI3K/AKT signaling pathway. *J Fluoresc*. 2023;33(4):1537–1557. doi:10.1007/S10895-023-03169-4/METRICS
11. Darban RA, Shareghi B, Asoodeh A, Chamani J. Multi-spectroscopic and molecular modeling studies of interaction between two different angiotensin I converting enzyme inhibitory peptides from gluten hydrolysate and human serum albumin. *J Biomol Struct Dyn*. 2016;35(16):3648–3662. doi:10.1080/07391102.2016.1264892
12. Khashkhashi-Moghadam S, Soleimani S, Bazanjani A, et al. Fabrication of versatile and sustainable cellulose nanocrystals from lettuce stalks as potential tamoxifen delivery vehicles for breast cancer treatment: biophysical, cellular and theoretical studies. *New J Chem*. 2023;47(31):14768–14791. doi:10.1039/D3NJ02388E
13. Sharifi-Rad A, Mehrzad J, Darroudi M, Saberi MR, Chamani J. Oil-in-water nanoemulsions comprising Berberine in olive oil: biological activities, binding mechanisms to human serum albumin or holo-transferrin and QMMD simulations. *J Biomol Struct Dyn*. 2020;39(3):1029–1043. doi:10.1080/07391102.2020.1724568
14. Patel D, Shukla S, Gupta S. Apigenin and cancer chemoprevention: progress, potential and promise. *Int J Oncol*. 2007;30(1):233–245. doi:10.3892/IJO.30.1.233/HTML
15. Shukla S, Gupta S. Apigenin: a promising molecule for cancer prevention. *Pharm Res*. 2010;27(6):962–978. doi:10.1007/S11095-010-0089-7
16. Yan X, Qi M, Li P, Zhan Y, Shao H. Apigenin in cancer therapy: anti-cancer effects and mechanisms of action. *Cell Biosci*. 2017;7(1):1–16. doi:10.1186/s13578-017-0179-x
17. Zhang J, Liu D, Huang Y, Gao Y, Qian S. Biopharmaceutics classification and intestinal absorption study of apigenin. *Int J Pharm*. 2012;436(1–2):311–317. doi:10.1016/J.IJPHARM.2012.07.002
18. Raj S, Khurana S, Choudhari R, et al. Specific targeting cancer cells with nanoparticles and drug delivery in cancer therapy. *Semin Cancer Biol*. 2021;69:166–177. doi:10.1016/J.SEMCANCER.2019.11.002
19. Thi TTH, Suys EJA, Lee JS, Nguyen DH, Park KD, Truong NP. Lipid-based nanoparticles in the clinic and clinical trials: from cancer nanomedicine to COVID-19 vaccines. *Vaccines*. 2021;9(4):359. doi:10.3390/VACCINES9040359
20. Dadwal A, Baldi A, Kumar Narang R. Nanoparticles as carriers for drug delivery in cancer. *Artif Cells Nanomed Biotechnol*. 2018;46:295–305. doi:10.1080/21691401.2018.1457039
21. García-Pinel B, Porras-Alcalá C, Ortega-Rodríguez A, et al. Lipid-based nanoparticles: application and recent advances in cancer treatment. *Nanomaterials*. 2019;9(4):638. doi:10.3390/NANO9040638
22. Bonilla L, Espina M, Severino P, et al. Lipid nanoparticles for the posterior eye segment. *Pharmaceutics*. 2022;14(1):90. doi:10.3390/PHARMACEUTICS14010090
23. Haider M, Abdin SM, Kamal L, Orive G. Nanostructured lipid carriers for delivery of chemotherapeutics: a review. *Pharmaceutics*. 2020;12(3):288. doi:10.3390/PHARMACEUTICS12030288
24. Bhave A, Schulzova V, Chmelarova H, Mrnka L, Hajslova J. Assessment of rosehips based on the content of their biologically active compounds. *J Food Drug Anal*. 2017;25(3):681–690. doi:10.1016/J.JFDA.2016.12.019

25. Mármol I, Sánchez-De-Diego C, Jiménez-Moreno N, Ancín-Azpilicueta C, Rodríguez-Yoldi M. Therapeutic applications of rose hips from different Rosa species. *Int J Mol Sci*. 2017;18(6):1137. doi:10.3390/IJMS18061137
26. Ayati Z, Amiri MS, Ramezani M, Delshad E, Sahebkar A, Emami SA. Phytochemistry, traditional uses and pharmacological profile of rose Hip: a review. *Curr Pharm Des*. 2018;24(35):4101–4124. doi:10.2174/1381612824666181010151849
27. Strugała P, Gładkowski W, Kucharska AZ, Sokół-łetowska A, Gabrielska J. Antioxidant activity and anti-inflammatory effect of fruit extracts from blackcurrant, chokeberry, hawthorn, and rosehip, and their mixture with linseed oil on a model lipid membrane. *Eur J Lipid Sci Technol*. 2016;118 (3):461–474. doi:10.1002/EJLT.201500001
28. Carvajal-Vidal P, Fábrega MJ, Espina M, Calpena AC, García ML. Development of Halobetasol-loaded nanostructured lipid carrier for dermal administration: optimization, physicochemical and biopharmaceutical behavior, and therapeutic efficacy. *Nanomed Nanotechnol Biol Med*. 2019;20:102026. doi:10.1016/J.NANO.2019.102026
29. Teeranachaideekul V, Boonme P, Souto EB, Müller RH, Junyaprasert VB. Influence of oil content on physicochemical properties and skin distribution of Nile red-loaded NLC. *J Control Release*. 2008;128(2):134–141. doi:10.1016/J.JCONREL.2008.02.011
30. Elmsmari F, González Sánchez JA, Duran-Sindreu F, et al. Calcium hydroxide-loaded PLGA biodegradable nanoparticles as an intracanal medicament. *Int Endod J*. 2021;54(11):2086–2098. doi:10.1111/IEJ.13603
31. Sánchez-López E, Ettcheto M, Egea MA, et al. Memantine loaded PLGA PEGylated nanoparticles for Alzheimer's disease: in vitro and in vivo characterization. *J Nanobiotechnology*. 2018;16(1):1–16. doi:10.1186/S12951-018-0356-Z/FIGURES/9
32. Sánchez-López E, Esteruelas G, Ortiz A, et al. Dexibuprofen biodegradable nanoparticles: one step closer towards a better ocular interaction study. *Nanomaterials*. 2020;10(4). doi:10.3390/NANO10040720
33. Gomathy S, Narenderan ST, Meyyanathan SN, Gowramma B. Development and validation of HPLC method for the simultaneous estimation of Apigenin andLuteolin in commercial formulation. *Artic J Crit Rev*. 2020;7(19):4785. doi:10.31838/jcr.07.19.560
34. Esteruelas G, Halbaut L, García-Torra V, et al. Development and optimization of Riluzole-loaded biodegradable nanoparticles incorporated in a mucoadhesive in situ gel for the posterior eye segment. *Int J Pharm*. 2022;612:121379. doi:10.1016/j.ijpharm.2021.121379
35. Cano A, Ettcheto M, Chang JH, et al. Dual-drug loaded nanoparticles of Epigallocatechin-3-gallate (EGCG)/Ascorbic acid enhance therapeutic efficacy of EGCG in a APPswe/PS1dE9 Alzheimer's disease mice model. *J Control Release*. 2019;301:62–75. doi:10.1016/J.JCONREL.2019.03.010
36. Liu P, De Wulf O, Laru J, et al. Dissolution studies of poorly soluble drug nanosuspensions in non-sink conditions. *AAPS PharmSciTech*. 2013;14 (2):748. doi:10.1208/S12249-013-9960-2
37. Esteruelas G, Souto EB, Espina M, et al. Diclofenac loaded biodegradable nanoparticles as antitumoral and antiangiogenic therapy. *Pharmaceutics*. 2022;15(1):102. doi:10.3390/PHARMACEUTICS15010102
38. Czarnecka M, Switalska M, Wietrzyk J, Maciejewska G, Gliszczyńska A. Synthesis and biological evaluation of phosphatidylcholines with cinnamic and 3-methoxycinnamic acids with potent antiproliferative activity. *RSC Adv*. 2018;8(62):35752. doi:10.1039/C8RA07002D
39. Nevozhay D. Cheburator software for automatically calculating drug inhibitory concentrations from in vitro screening assays. *PLoS One*. 2014;9 (9):e106186. doi:10.1371/JOURNAL.PONE.0106186
40. Zeb A, Qureshi OS, Kim HS, et al. High payload itraconazole-incorporated lipid nanoparticles with modulated release property for oral and parenteral administration. *J Pharm Pharmacol*. 2017;69(8):955–966. doi:10.1111/JPHP.12727
41. Khan AA, Abdulbaqi IM, Abou Assi R, Murugaiyah V, Darwis Y. Lyophilized hybrid nanostructured lipid carriers to enhance the cellular uptake of verapamil: statistical optimization and in vitro evaluation. *Nanoscale Res Lett*. 2018;13:323. doi:10.1186/S11671-018-2744-6
42. Folle C, Marqués AM, Díaz-Garrido N, et al. Thymol-loaded PLGA nanoparticles: an efficient approach for acne treatment. *J Nanobiotechnology*. 2021;19(1):359. doi:10.1186/S12951-021-01092-Z
43. Bunjes H, Westesen K, Koch MHJ. Crystallization tendency and polymorphic transitions in triglyceride nanoparticles. *Int J Pharm*. 1996;129(1–2):159–173. doi:10.1016/0378-5173(95)04286-5
44. Souto EB, Mehnert W, Müller RH. Polymorphic behaviour of Compritol 888 ATO as bulk lipid and as SLN and NLC. *J Microencapsul*. 2006;23 (4):417–433. doi:10.1080/02652040600612439
45. Alshehri SM, Shakeel F, Ibrahim MA, et al. Dissolution and bioavailability improvement of bioactive apigenin using solid dispersions prepared by different techniques. *Saudi Pharm J*. 2019;27(2):264–273. doi:10.1016/J.JSPS.2018.11.008
46. Pápay ZE, Kósa A, Böddi B, et al. Study on the pulmonary delivery system of Apigenin-loaded albumin nanocarriers with antioxidant activity. *J Aerosol Med Pulm Drug Deliv*. 2017;30(4):274–288. doi:10.1089/JAMP.2016.1316
47. Freitas C, Müller RH. Correlation between long-term stability of solid lipid nanoparticles (SLN) and crystallinity of the lipid phase. *Eur J Pharm Biopharm*. 1999;47(2):125–132. doi:10.1016/S0939-6411(98)00074-5
48. Zimmermann E, Souto EB, Müller RH. Physicochemical investigations on the structure of drug-free and drug-loaded solid lipid nanoparticles (SLN) by means of DSC and 1H NMR. *Pharmazie*. 2005;60(7):508–513.
49. Stability of Dispersions | 3P Instruments. Available from: https://www.3p-instruments.com/measurement-methods/stability-turbiscan/. Accessed November 22, 2021.
50. Anwer MK, Mohammad M, Ezzeldin E, Fatima F, Alalaiwe A, Iqbal M. Preparation of sustained release apremilast-loaded PLGA nanoparticles: in vitro characterization and in vivo pharmacokinetic study in rats. *Int J Nanomedicine*. 2019;14:1595. doi:10.2147/IJN.S195048
51. Tapeinos C, Battaglini M, Ciofani G. Advances in the design of solid lipid nanoparticles and nanostructured lipid carriers for targeting brain diseases. *J Control Release*. 2017;264:306–332. doi:10.1016/J.JCONREL.2017.08.033
52. Amasya G, Aksu B, Badilli U, Onay-Besikci A, Tarimci N. QbD guided early pharmaceutical development study: production of lipid nanoparticles by high pressure homogenization for skin cancer treatment. *Int J Pharm*. 2019;563:110–121. doi:10.1016/J.IJPHARM.2019.03.056
53. Bahari LAS, Hamishehkar H. The impact of variables on particle size of solid lipid nanoparticles and nanostructured lipid carriers; a comparative literature review. *Adv Pharm Bull*. 2016;6(2):151. doi:10.15171/APB.2016.021
54. Oh KS, Kim RS, Lee J, Kim D, Cho SH, Yuk SH. Gold/chitosan/pluronic composite nanoparticles for drug delivery. *J Appl Polym Sci*. 2008;108 (5):3239–3244. doi:10.1002/APP.27767
55. Seo Y, Lim H, Park H, et al. Recent progress of lipid nanoparticles-based lipophilic drug delivery: focus on surface modifications. *Pharmaceutics*. 2023;15(3):772. doi:10.3390/PHARMACEUTICS15030772

56. Kazmi I, Al-Abbasi FA, Imam SS, et al. Formulation and evaluation of Apigenin-loaded hybrid nanoparticles. *Pharmaceutics*. 2022;14(4):783. doi:10.3390/PHARMACEUTICS14040783
57. Mahmoudi S, Ghorbani M, Sabzichi M, Ramezani F, Hamishehkar H, Samadi N. Targeted hyaluronic acid-based lipid nanoparticle for apigenin delivery to induce Nrf2-dependent apoptosis in lung cancer cells. *J Drug Deliv Sci Technol*. 2019;49:268–276. doi:10.1016/J.JDDST.2018.11.013
58. Gilani SJ, Bin-jumah MN, Imam SS, Alshehri S, Jahangir MA, Zafar A. Formulation and optimization of nano lipid based oral delivery systems for arthritis. *Coatings*. 2021;11(5):548. doi:10.3390/COATINGS11050548
59. Liu L, Tang Y, Gao C, et al. Characterization and biodistribution in vivo of quercetin-loaded cationic nanostructured lipid carriers. *Colloids Surfaces B Biointerfaces*. 2014;115:125–131. doi:10.1016/J.COLSURFB.2013.11.029
60. Ojo AT, Ma C, Lee PI. Elucidating the effect of crystallization on drug release from amorphous solid dispersions in soluble and insoluble carriers. *Int J Pharm*. 2020;591:120005. doi:10.1016/J.IJPHARM.2020.120005
61. Huang Z, Ma C, Wu M, et al. Exploring the drug-lipid interaction of weak-hydrophobic drug loaded solid lipid nanoparticles by isothermal titration calorimetry. *J Nanoparticle Res*. 2020;22(1):1–14. doi:10.1007/S11051-019-4671-6/METRICS
62. Pochapski DJ, Carvalho Dos Santos C, Leite GW, Pulcinelli SH, Santilli CV. Zeta Potential and colloidal stability predictions for inorganic nanoparticle dispersions: effects of experimental conditions and electrokinetic models on the interpretation of results. *Langmuir*. 2021;37(45):13379–13389. doi:10.1021/ACS.LANGMUIR.1C02056
63. Kan KHM, Li J, Wijesekera K, Cranston ED. Polymer-grafted cellulose nanocrystals as pH-responsive reversible flocculants. *Biomacromolecules*. 2013;14(9):3130–3139. doi:10.1021/BM400752K
64. Hoare SRJ. Analyzing kinetic binding data. Assay Guidance Manual; 2021. Avaiable from: https://www.ncbi.nlm.nih.gov/books/NBK569501/. Accessed September 7, 2023.
65. Chamani J, Moosavi-Movahedi AA, Hakimelahi GH. Structural changes in β-lactoglobulin by conjugation with three different kinds of carboxymethyl cyclodextrins. *Thermochim Acta*. 2005;432(1):106–111. doi:10.1016/J.TCA.2005.04.014
66. Hosseinzadeh M, Nikjoo S, Zare N, Delavar D, Beigoli S, Chamani J. Characterization of the structural changes of human serum albumin upon interaction with single-walled and multi-walled carbon nanotubes: spectroscopic and molecular modeling approaches. *Res Chem Intermed*. 2019;45(2):401–423. doi:10.1007/S11164-018-3608-5/METRICS
67. Mujtaba MA, Alotaibi NM, Alshehri SM, et al. Novel therapeutic approach in PEGylated chitosan nanoparticles of Apigenin for the treatment of cancer via oral nanomedicine. *Polymers (Basel)*. 2022;14(20):4344. doi:10.3390/POLYM14204344
68. Zoubari G, Staufenbiel S, Volz P, Alexiev U, Bodmeier R. Effect of drug solubility and lipid carrier on drug release from lipid nanoparticles for dermal delivery. *Eur J Pharm Biopharm*. 2017;110:39–46. doi:10.1016/J.EJPB.2016.10.021
69. Alfaleh MA, Hashem AM, Abujamel TS, et al. Apigenin loaded Lipoid–PLGA–TPGS nanoparticles for colon cancer therapy: characterization, sustained release, cytotoxicity, and apoptosis pathways. *Polymers (Basel)*. 2022;14(17):3577. doi:10.3390/POLYM14173577/S1
70. Imran M, Aslam Gondal T, Atif M, et al. Apigenin as an anticancer agent. *Phyther Res*. 2020;34(8):1812–1828. doi:10.1002/PTR.6647
71. Sun D, Liu Y, Yu Q, et al. The effects of luminescent ruthenium(II) polypyridyl functionalized selenium nanoparticles on bFGF-induced angiogenesis and AKT/ERK signaling. *Biomaterials*. 2013;34(1):171–180. doi:10.1016/J.BIOMATERIALS.2012.09.031
72. Fu J, Zeng W, Chen M, et al. Apigenin suppresses tumor angiogenesis and growth via inhibiting HIF-1α expression in non-small cell lung carcinoma. *Chem Biol Interact*. 2022;361:109966. doi:10.1016/J.CBI.2022.109966
73. Gunasekaran T, Haile T, Nigusse T, Dhanaraju MD. Nanotechnology: an effective tool for enhancing bioavailability and bioactivity of phytomedicine. *Asian Pac J Trop Biomed*. 2014;4(Suppl 1):S7. doi:10.12980/APJTB.4.2014C980
74. Chen L, Wang S, Feng Y, et al. Utilisation of chick embryo chorioallantoic membrane as a model platform for imaging-navigated biomedical research. *Cells*. 2021;10(2):1–41. doi:10.3390/CELLS10020463
75. Kim TJ, Zhang YH, Kim Y, et al. Effects of apigenin on the serum- and platelet derived growth factor-BB-induced proliferation of rat aortic vascular smooth muscle cells. *Planta Med*. 2002;68(7):605–609. doi:10.1055/S-2002-32901
76. Fang J, Xia C, Cao Z, Zheng JZ, Reed E, Jiang B-H. Apigenin inhibits VEGF and HIF-1 expression via PI3K/AKT/p70S6K1 and HDM2/p53 pathways. *FASEB J*. 2005;19(3):342–353. doi:10.1096/FJ.04-2175COM
77. Lee WJ, Chen WK, Wang CJ, Lin WL, Tseng TH. Apigenin inhibits HGF-promoted invasive growth and metastasis involving blocking PI3K/Akt pathway and beta 4 integrin function in MDA-MB-231 breast cancer cells. *Toxicol Appl Pharmacol*. 2008;226(2):178–191. doi:10.1016/J.TAAP.2007.09.013
78. El-Kenawi AE, El-Remessy AB. Angiogenesis inhibitors in cancer therapy: mechanistic perspective on classification and treatment rationales. *Br J Pharmacol*. 2013;170(4):729. doi:10.1111/BPH.12344
79. Ruela-De-Sousa RR, Fuhler GM, Blom N, Ferreira CV, Aoyama H, Peppelenbosch MP. Cytotoxicity of apigenin on leukemia cell lines: implications for prevention and therapy. *Cell Death Dis*. 2010;1. doi:10.1038/cddis.2009.18
80. Behzadi S, Serpooshan V, Tao W, et al. Cellular uptake of nanoparticles: journey inside the cell. *Chem Soc Rev*. 2017;46(14):4244. doi:10.1039/C6CS00636A
81. Wojtowicz W, Wróbel A, Pyziak K, et al. Evaluation of MDA-MB-468 cell culture media analysis in predicting triple-negative breast cancer patient sera metabolic profiles. *Metabolites*. 2020;10(5):173. doi:10.3390/METABO10050173
82. Bauer D, Mazzio E, Hilliard A, Oriaku ET, Soliman KFA. Effect of apigenin on whole transcriptome profile of TNFα–activated MDA–MB–468 triple negative breast cancer cells. *Oncol Lett*. 2020;19(3):2123–2132. doi:10.3892/OL.2020.11327/HTML
83. Way TD, Kao MC, Lin JK. Apigenin induces apoptosis through proteasomal degradation of HER2/neu in HER2/neu-overexpressing breast cancer cells via the phosphatidylinositol 3-kinase/Akt-dependent pathway. *J Biol Chem*. 2004;279(6):4479–4489. doi:10.1074/JBC.M305529200
84. Bai H, Jin H, Yang F, Zhu H, Cai J. Apigenin induced MCF-7 cell apoptosis-associated reactive oxygen species. *Scanning*. 2014;36(6):622–631. doi:10.1002/SCA.21170
85. Calderón-Montaño JM, Martínez-Sánchez SM, Jiménez-González V, et al. Screening for selective anticancer activity of 65 extracts of plants collected in western Andalusia, Spain. *Plants*. 2021;10(10):2193. doi:10.3390/PLANTS10102193/S1
86. Badr-Eldin SM, Aldawsari HM, Ahmed OAA, et al. Optimized semisolid self-nanoemulsifying system based on glyceryl behenate: a potential nanoplatform for enhancing antitumor activity of raloxifene hydrochloride in MCF-7 human breast cancer cells. *Int J Pharm*. 2021;600:120493. doi:10.1016/J.IJPHARM.2021.120493

87. Khuda SE, Nguyen AV, Sharma GM, Alam MS, Balan KV, Williams KM. Effects of emulsifiers on an in vitro model of intestinal epithelial tight junctions and the transport of food allergens. *Mol Nutr Food Res*. 2022;66(4):e2100576. doi:10.1002/MNFR.202100576
88. Ilyasoğlu H, Ilyaso H. Characterization of rosehip (Rosa canina L.) seed and seed oil. *Int J Food Prop*. 2014;17(7):1591–1598. doi:10.1080/10942912.2013.777075
89. Mármol I, Jiménez-Moreno N, Ancín-Azpilicueta C, Osada J, Cerrada E, Rodríguez-Yoldi MJ. A combination of Rosa Canina extracts and gold complex favors apoptosis of Caco-2 cells by increasing oxidative stress and mitochondrial dysfunction. *Antioxidants*. 2019;9(1):17. doi:10.3390/ANTIOX9010017
90. Cagle P, Idassi O, Carpenter J, Minor R, Goktepe I, Martin P. Effect of rosehip (Rosa Canina) extracts on human brain tumor cell proliferation and apoptosis. *J Cancer Ther*. 2012;2012(5):534–545. doi:10.4236/JCT.2012.35069
91. Federation of American Societies for Experimental Biology (FASEB). Natural extract shows promise for preventing breast cancer, study suggests – ScienceDaily; 2015. Avaiable from: https://www.sciencedaily.com/releases/2015/03/150329141007.htm. Accessed May 14, 2023.
92. Neves AR, Queiroz JF, Costa Lima SA, Figueiredo F, Fernandes R, Reis S. Cellular uptake and transcytosis of lipid-based nanoparticles across the intestinal barrier: relevance for oral drug delivery. *J Colloid Interface Sci*. 2016;463:258–265. doi:10.1016/J.JCIS.2015.10.057
93. Jeitler R, Glader C, Tetyczka C, et al. Investigation of cellular interactions of lipid-structured nanoparticles with oral mucosal epithelial cells. *Front Mol Biosci*. 2022;9:554. doi:10.3389/FMOLB.2022.917921/BIBTEX